Estimation of satellite and receiver biases on multiple Galileo frequencies with a Kalman filter

P. Henkel*, Z. Wen* and C. Günther*,**
*Technische Universität München (TUM), Munich, Germany
**German Aerospace Center (DLR), Oberpfaffenhofen, Germany

BIOGRAPHIES

Patrick Henkel studied electrical engineering and information technology at the Technische Universität München, Munich, Germany, and the École Polytechnique de Montréal, Montréal, QC, Canada. He is currently finalizing his Ph.D. thesis at the Institute of Communications and Navigation, TUM, and his focus is on robust ambiguity resolution for precise carrier-phase positioning with multiple frequencies.

In 2007, he was a Guest Researcher at TU Delft, in 2008 at the GPS Lab at Stanford University, Stanford, CA. Mr. Henkel received the Pierre Contensou Gold Medal at the International Astronautical Congress in 2007.

Zhibo Wen has received his bachelor degree from Shanghai Jiao Tong University, China. Since 2008, he is studying Electrical Engineering and Information Technology at the Technische Universitat Munchen, Germany, with a specialization on communication technology. He is currently working on his Master thesis on phase and code bias estimation with a Kalman filter for satellite based augmentation systems.

Christoph Günther studied theoretical physics at the Swiss Federal Institute of Technology in Zurich. He received his diploma in 1979 and completed his PhD in 1984. He worked on communication and information theory at Brown Boveri and Ascom Tech. From 1995, he led the development of mobile phones for GSM and later dual mode GSM/Satellite phones at Ascom. In 1999, he became head of the research department of Ericsson in Nuremberg. Since 2003, he is the director of the Institute of Communication and Navigation at the German Aerospace Center (DLR) and since December 2004, he additionally holds a Chair at the Technische Universität München (TUM). His research interests are in satellite navigation, communication and signal processing.

ABSTRACT

Reliable integer ambiguity resolution requires precise bias estimates for absolute positioning. In this paper, a method for the joint estimation of satellite code, satellite phase, receiver code and receiver phase biases on multiple frequencies is proposed. It uses a Kalman filter and sequential bootstrapping for integer ambiguity resolution. The reliability of ambiguity resolution is improved by an integer decorrelation transformation. The achievable bias accuracies, the benefit of ambiguity resolution and the benefit of measurements on a third frequency is shown for a global network of reference stations.

Moreover, a second method is suggested for the joint estimation of code biases and grid ionospheric vertical delays. Code measurements on two frequencies and two linear combinations of time-differenced carrier phase measurements are used in a Kalman filter. The ionospheric delays at the grid points are obtained by a least-squares fitting of the ionospheric slant delays at the surrounding pierce points.

The method is validated from both simulated measurements of the EGNOS RIMS stations and from real data.

INTRODUCTION

Carrier phase measurements are extremely accurate but ambiguous. Precise point positioning with integer ambiguity resolution requires precise bias estimates. These biases can be split into receivers biases (e.g. hardware delays) and satellite biases including orbital errors, satellite clock offsets, phase center variations and phase wind-up.

Ge et al. [1], Gabor and Nerem [2] and Laurichesse and Mercier [3] have tried to estimate the L1 phase and code biases. The derivation is briefly introduced here and starts with the geometry-free, ionosphere-free Melbourne-Wübbena combination [4]. It combines the phase measurements ϕ_1, ϕ_2 (in units of cycles) and the code measurements ρ_1 and ρ_2 on the frequencies f_1 and f_2 as

$$\left(\frac{f_1}{f_1-f_2}\lambda_1\phi_1 - \frac{f_2}{f_1-f_2}\lambda_2\phi_2\right) - \left(\frac{f_1}{f_1+f_2}\rho_1 + \frac{f_2}{f_1+f_2}\rho_2\right) = \lambda_{\mathrm{w}} b_{\mathrm{w}} + \varepsilon_{\mathrm{w}}, \quad (1)$$

with the widelane wavelength

$$\lambda_{\mathrm{w}} = \frac{1}{\frac{1}{\lambda_1} - \frac{1}{\lambda_2}}, \quad (2)$$

the combined ambiguity/ bias term

$$b_{\mathrm{w}} = N_1 - N_2 + b_{\phi_1} - b_{\phi_2} - \frac{f_1-f_2}{f_1+f_2}\cdot\frac{b_{\rho_1}}{\lambda_1} - \frac{f_1-f_2}{f_1+f_2}\cdot\frac{b_{\rho_2}}{\lambda_2}, \quad (3)$$

where N_1 and N_2 are integer ambiguities, and ε_{w} represents the combined phase and code noise.

In a second step, the geometry-preserving, ionosphere-free phase only combination is computed, i.e.

$$\frac{f_1^2}{f_1^2-f_2^2}\lambda_1\phi_1 - \frac{f_2^2}{f_1^2-f_2^2}\lambda_2\phi_2 = g + b_{\mathrm{c}} + \varepsilon_{\mathrm{c}} \quad (4)$$

with the geometry g including the range and some non-dispersive errors that are introduced in the next section, and the combined ambiguity/ bias term

$$b_{\mathrm{c}} = \frac{f_1^2}{f_1^2-f_2^2}\cdot\lambda_1(N_1+b_{\phi_1}) - \frac{f_2^2}{f_1^2-f_2^2}\cdot\lambda_2(N_2+b_{\phi_2}). \quad (5)$$

The biases of the Melbourne-Wübbena combination and of the ionosphere-free combination are combined into

$$\frac{f_1+f_2}{c}\cdot b_{\mathrm{c}} - \frac{f_2}{f_1-f_2}\cdot b_{\mathrm{w}} = N_1 + \tilde{b}_{\phi_1} \quad (6)$$

with

$$\tilde{b}_{\phi_1} = b_{\phi_1} + \frac{f_2}{f_1+f_2}\cdot\frac{b_{\rho_1}}{\lambda_1} + \frac{f_2}{f_1+f_2}\cdot\frac{b_{\rho_2}}{\lambda_2}. \quad (7)$$

Similarly, an estimate of the phase bias on the second frequency can be obtained as

$$\tilde{b}_{\phi_2} = b_{\phi_2} + \frac{f_1}{f_1+f_2}\cdot\frac{b_{\rho_1}}{\lambda_1} + \frac{f_1}{f_1+f_2}\cdot\frac{b_{\rho_2}}{\lambda_2}. \quad (8)$$

The transmission of $\tilde{b}_{\phi_1}$ and $\tilde{b}_{\phi_2}$ enables an unbiased estimation of L1 and L2 integer ambiguities at the mobile receiver. However, these phase biases also include a weighted combination of code biases on both frequencies. It can be shown that these L1/ L2 pseudo-phase biases correspond to a geometry-preserving, ionosphere-free narrowlane combination with a wavelength of only 10.7 cm. There does not exist any geometry-preserving, ionosphere-free combination with the applicability of these biases and a larger wavelength than 10.7 cm. Moreover, a substantial code noise can be observed in the narrowlane combinations.

In this paper, an alternative approach is suggested to overcome these shortcomings. A Kalman filter is used to estimate satellite code, satellite phase, receiver code and receiver phase biases on multiple frequencies. The integer ambiguities are resolved sequentially after integer decorrelation by bootstrapping. A probability of wrong fixing of 10^{-9} is achievable. The use of measurements on a third frequency enables an even earlier ambiguity fixing. The fixing results in a substantial reduction of the bias uncertainties.

Additionally, a second method is suggested for the joint estimation of code biases and grid ionospheric vertical delays (GIVD). These GIVDs are obtained from a least-squares fitting of the slant ionospheric delays at the surrounding pierce points. The method is validated from both simulated measurements and real data.

MEASUREMENT MODEL

The code and carrier phase measurements in units of meters on two frequencies of satellite k, receiver r and epoch t_n are modeled as

$$\begin{aligned}
\rho_{1,r}^k(t_n) &= g_r^k(t_n) + I_{1,r}^k(t_n) + b_{1,r} + b_1^k + \eta_{1,r}^k(t_n) \\
\rho_{2,r}^k(t_n) &= g_r^k(t_n) + q_{12}^2 I_{1,r}^k(t_n) \\
&\quad + b_{2,r} + b_2^k + \eta_{2,r}^k(t_n) \\
\lambda_1\phi_{1,r}^k(t_n) &= g_r^k(t_n) - I_{1,r}^k(t_n) + \lambda_1 N_{1,r}^k \\
&\quad + \beta_{1,r} + \beta_1^k + \varepsilon_{1,r}^k(t_n) \\
\lambda_2\phi_{2,r}^k(t_n) &= g_r^k(t_n) - q_{12}^2 I_{1,r}^k(t_n) + \lambda_2 N_{2,r}^k \\
&\quad + \beta_{2,r} + \beta_2^k + \varepsilon_{2,r}^k(t_n),
\end{aligned} \quad (9)$$

where g_r denotes the geometry term, $I_{1,r}^k$ is the slant ionospheric delay, $q_{12} = f_1/f_2$ is the ratio of frequencies, $N_{m,r}^k$ is the integer ambiguity on frequency f_m, $\beta_{m,r}$ is the receiver phase bias, β_m^k is the satellite phase bias, $b_{m,r}$ is the receiver code bias, b_m^k is the satellite code bias, $\eta_{m,r}^k$ is the code noise and $\varepsilon_{m,r}^k$ is the phase noise including multipath on frequency $m = \{1, 2\}$.

A dynamical model is used for the geometry term $g_r^k(t_n)$ which can be split into the range r_r^k, clock offsets $c\delta\tau_r$ and $c\delta\tau^k$ and tropospheric delays T_r^k, i.e.

$$\begin{aligned}
g_r^k(t_n) &= g_r^k(t_{n-1}) + \Delta t \cdot \dot{g}_r^k(t_{n-1}) + w_{g_r^k}(t_n) \\
&= r_r^k(t_n) + c\cdot(\delta\tau_r(t_n) - \delta\tau^k) + T_r^k(t_n),
\end{aligned} \quad (10)$$

where $w_{g_r^k}(t_n) \sim \mathcal{N}(0, \sigma^2_{w_{g_r^k}})$ denotes the process noise to model accelerations. The slant ionospheric delay $I_{1,r}^k$ is rewritten as

$$I_{1,r}^k(t_n) = m_{\mathrm{I}}(E_r^k(t_n)) \cdot I_{\mathrm{v}}(t_n), \quad (11)$$

with the vertical ionospheric delay I_{v} at the ionospheric pierce point (IPP) and the mapping function m_{I} that is given by

$$m_{\mathrm{I}}(E_r^k(t_n)) = \frac{1}{\sqrt{1-\frac{\cos^2(E_r^k(t_n))}{(1+h/R_{\mathrm{e}})^2}}}, \tag{12}$$

with the elevation angle $E_r^k(t_n)$ and the height h of the ionospheric shell above the ground.

The phase and code noise is assumed to follow a zero mean white Gaussian distribution. The standard deviations $\sigma_{\rho_{m,r}^k}$ of the code tracking errors have been set to the Cramer Rao bounds that are shown in Table 1 for the wideband Galileo signals at a carrier to noise power ratio of 45dBHz [5]. The phase noise standard deviations $\sigma_{\phi_{m,r}^k}$ have been assumed to be 1 mm.

Table 1 Cramer Rao Bounds for $C/N_0 = 45\mathrm{dBHz}$

	Signal	BW [MHz]	Γ [cm]
E1	MBOC	20	11.14
E5	AltBOC(15,10)	51	1.95
E5a	BPSK(10)	20	7.83
E5b	BPSK(10)	20	7.83

PARAMETER MAPPING

The estimation of all biases in Eq. (9) is not feasible but also not required as some biases can not be separated from the remaining parameters. Additionally, the integer ambiguity resolution is simplified if the code biases are mapped to the ranges and ionospheric delays, i.e.

$$\begin{aligned} &g_r^k(t_n) + q_{11}^2 I_r^k(t_n) + b_{1,r} + b_1^k \\ &= \underbrace{\left(g_r^k + b_{g_r} + b_{g^k}\right)}_{\tilde{g}_r^k(t_n)} + q_{11}^2 \underbrace{\left(I_r^k(t_n) + b_{I_r} + b_{I^k}\right)}_{\tilde{I}_r^k(t_n)} \end{aligned} \tag{13}$$

and

$$\begin{aligned} &g_r^k(t_n) + q_{12}^2 I_r^k(t_n) + b_{2,r} + b_2^k \\ &= \left(g_r^k + b_{g_r} + b_{g^k}\right) + q_{12}^2 \left(I_r^k(t_n) + b_{I_r} + b_{I^k}\right). \end{aligned} \tag{14}$$

Equations (13) and (14) can be solved for the receiver dependant biases b_{g_r} and b_{I_r} which can be expressed as a function of $b_{1,r}$ and $b_{2,r}$, i.e.

$$b_{g_r} = -\frac{b_{2,r} - q_{12}^2 b_{1,r}}{q_{12}^2 - 1}, \quad b_{I_r} = -\frac{b_{1,r} - b_{2,r}}{q_{12}^2 - 1}. \tag{15}$$

Similarly, the satellite dependant biases b_g^k and b_I^k are given by

$$b_{g^k} = -\frac{b_2^k - q_{12}^2 b_1^k}{q_{12}^2 - 1}, \quad b_{I^k} = -\frac{b_1^k - b_2^k}{q_{12}^2 - 1}. \tag{16}$$

Moreover, the satellite phase biases of one satellite can be absorbed by the receiver phase biases, i.e.

$$\begin{aligned} \tilde{\beta}_{1,r} &= \beta_{1,r} + \beta_1^1, \quad \tilde{\beta}_1^k = \beta_1^k - \beta_1^1 \\ \tilde{\beta}_{2,r} &= \beta_{2,r} + \beta_2^1, \quad \tilde{\beta}_2^k = \beta_2^k - \beta_2^1. \end{aligned} \tag{17}$$

There are $R+K-1$ remaining phase biases $\tilde{\beta}_{m,r}$ and $\tilde{\beta}_m^k$ on each frequency which can not be separated from the ambiguities and, thus, are absorbed by $R+K-1$ ambiguities. However, the number of all ambiguities is $s = \sum_{r=1}^R K_r$ on each frequency (with K_r being the number of visible satellites for the r-th reference station) which results in two subset of ambiguities: One subset which includes float valued ambiguities, and one which includes integer valued ambiguities. The latter one is in general much larger than the first one. The choice of the subset of integer ambiguities offers some additional degrees of freedom. It is suggested to choose the subset such that the error in the bias estimation is minimized.

ESTIMATION OF CODE AND CARRIER PHASE BIASES

The precise estimation of receiver and satellite biases requires a global network and a few hundred epochs which motivates a recursive state estimation, e.g. a Kalman filter [6]. The state vector includes the ranges, range rates, ionospheric delays, receiver and satellite phase biases and ambiguities, i.e.

$$\boldsymbol{x}_n = \left[\tilde{\boldsymbol{g}}^T(t_n),\ \dot{\boldsymbol{g}}^T(t_n),\ \tilde{\boldsymbol{I}}^T(t_n),\ \tilde{\boldsymbol{\beta}}_{\mathrm{R}}^T,\ \tilde{\boldsymbol{\beta}}_{\mathrm{S}}^T, \boldsymbol{N}\right]^T, \tag{18}$$

with

$$\begin{aligned} \tilde{\boldsymbol{g}}(t_n) &= \left[\tilde{g}_1^1(t_n), \ldots, \tilde{g}_1^{K_1}(t_n), \ldots, \tilde{g}_R^{K_R}(t_n)\right]^T \\ \dot{\boldsymbol{g}}(t_n) &= \left[\dot{g}_1^1(t_n), \ldots, \dot{g}_1^{K_1}(t_n), \ldots, \dot{g}_R^{K_R}(t_n)\right]^T \\ \tilde{\boldsymbol{I}}(t_n) &= \left[\tilde{I}_1^1(t_n), \ldots, \tilde{I}_1^{K_1}(t_n), \ldots, \tilde{I}_R^{K_R}(t_n)\right]^T \\ \tilde{\boldsymbol{\beta}}_{\mathrm{R}} &= \left[\tilde{\beta}_{1,1}, \ldots, \tilde{\beta}_{1,R}, \ldots, \tilde{\beta}_{2,1}, \ldots, \tilde{\beta}_{2,R}\right]^T \\ \tilde{\boldsymbol{\beta}}_{\mathrm{S}} &= \left[\tilde{\beta}_1^2, \ldots, \tilde{\beta}_1^K, \ldots, \tilde{\beta}_2^2, \ldots, \tilde{\beta}_2^K\right]^T, \end{aligned} \tag{19}$$

and the subset of integer valued ambiguities $\boldsymbol{N}$. The phase and code measurements of Eq. (9) are written in matrix-vector notation as

$$\begin{aligned} \boldsymbol{z}_n &= \Big[\phi_{1,1}^1(t_n), \ldots, \phi_{1,R}^{K_R}(t_n), \ldots, \phi_{2,R}^{K_R}(t_n), \\ &\quad\ \rho_{1,1}^1(t_n), \ldots, \rho_{1,R}^{K_R}(t_n), \ldots, \rho_{2,R}^{K_R}(t_n)\Big], \\ &= \boldsymbol{H}_n^{(1)} \boldsymbol{x}_n + \boldsymbol{v}_n, \end{aligned} \tag{20}$$

where $\boldsymbol{H}_n^{(1)}$ is implicitly given by Eq. (9), (10), (13), (14), (17), (18) and (19) and depends only on λ_1 and λ_2. The measurement noise $\boldsymbol{v}_n$ is assumed to be uncorrelated between satellites and zero-mean white Gaussian distributed with the variance $\sigma^2_{\phi_{m,r}^k}$ and $\sigma^2_{\rho_{m,r}^k}$. The state space model for $\boldsymbol{x}_n$ is given by

$$\boldsymbol{x}_n = \boldsymbol{\Phi} \boldsymbol{x}_{n-1} + \boldsymbol{w}_n, \tag{21}$$

with the state transition matrix

$$\boldsymbol{\Phi} = \begin{bmatrix} \mathbf{1}^{s\times s} & \Delta t \cdot \mathbf{1}^{s\times s} & \mathbf{0} \\ \mathbf{0} & \mathbf{1}^{s\times s} & \mathbf{0} \\ \mathbf{0} & \mathbf{0} & \mathbf{1}^{3s\times 3s} \end{bmatrix}, \tag{22}$$

where Δt represents the interval between two measurements. The process noise $\boldsymbol{w}_n \sim \mathcal{N}(\mathbf{0}, \boldsymbol{\Sigma}_\mathrm{w})$ is assumed to follow a Gaussian distribution. The state covariance matrix of range and range-rate related errors has been derived by Brown et al. in [6] and is given by

$$\boldsymbol{\Sigma}_{\mathrm{w},g\dot{g}} = \begin{bmatrix} S_p \cdot \Delta t^3/3 & S_p \cdot \Delta t^2/2 \\ S_p \cdot \Delta t^2/2 & S_p \cdot \Delta t \end{bmatrix} \otimes \mathbf{1}^{s\times s}, \tag{23}$$

which is used to model the covariance matrix of the whole state vector as

$$\boldsymbol{\Sigma}_\mathrm{w} = \begin{bmatrix} \boldsymbol{\Sigma}_{\mathrm{w},g\dot{g}} & & \\ & \boldsymbol{\Sigma}_{\mathrm{w},I} & \\ & & \boldsymbol{\Sigma}_{\mathrm{w},b} \end{bmatrix}, \tag{24}$$

with

$$\begin{aligned} \boldsymbol{\Sigma}_{\mathrm{w},I} &= \sigma_\mathrm{I}^2 \cdot \mathbf{1}^{s\times s} \\ \boldsymbol{\Sigma}_{\mathrm{w},b} &= \mathbf{0}^{2s\times 2s}, \end{aligned} \tag{25}$$

i.e. no process noise is assumed for the biases and integer ambiguities. In this work, the spectral amplitudes of the random walk processes have been set to $S_\mathrm{p} = 1$ m and $\sigma_I = 1$ cm.

The a posteriori state estimate $\hat{\boldsymbol{x}}_n^+$ is given by

$$\hat{\boldsymbol{x}}_n^+ = \hat{\boldsymbol{x}}_n^- + \boldsymbol{K}_n^{(1)} \left(\boldsymbol{z}_n - \boldsymbol{H}_n^{(1)} \hat{\boldsymbol{x}}_n^- \right), \tag{26}$$

with the Kalman gain $\boldsymbol{K}_n^{(1)}$ and the a priori state estimate $\hat{\boldsymbol{x}}_n^-$. The latter one is obtained by the prediction

$$\hat{\boldsymbol{x}}_n^- = \boldsymbol{\Phi} \hat{\boldsymbol{x}}_{n-1}^+, \tag{27}$$

with the covariance matrix

$$\boldsymbol{P}_{\hat{\boldsymbol{x}}_n^-} = \boldsymbol{\Phi} \boldsymbol{P}_{\hat{\boldsymbol{x}}_{n-1}^+} \boldsymbol{\Phi}^T + \boldsymbol{\Sigma}_\mathrm{w}. \tag{28}$$

The covariance matrix of the a posteriori state estimate is given by

$$\boldsymbol{P}_{\hat{\boldsymbol{x}}_n^+} = \left(\mathbf{1} - \boldsymbol{K}_n \boldsymbol{H}_n^{(1)} \right) \boldsymbol{P}_{\hat{\boldsymbol{x}}_n^-}. \tag{29}$$

The Kalman filter is initialized by a least-squares estimation from a few epochs.

The success rate of sequential ambiguity resolution ('bootstrapping') can be substantially improved by the integer ambiguity transformation $\boldsymbol{Z}$ of Teunissen [7]. It is applied to the float ambiguity estimates $\hat{\boldsymbol{N}}$ of the a posteriori state estimate $\hat{\boldsymbol{x}}_n^+$, i.e.

$$\hat{\boldsymbol{N}}' = \boldsymbol{Z} \hat{\boldsymbol{N}}. \tag{30}$$

The k-th conditional ambiguity estimate is given by

$$\begin{aligned} \hat{N}_{k|1,\ldots,k-1} &= \hat{N}_k - \sum_{j=1}^{k-1} \sigma_{\hat{N}_k \hat{N}_{j|1,\ldots,j-1}} \sigma^{-2}_{\hat{N}_{j|1,\ldots,j-1}} \\ &\quad \cdot \left(\hat{N}_{j|1,\ldots,j-1} - [\hat{N}_{j|1,\ldots,j-1}] \right), \end{aligned} \tag{31}$$

where $[\cdot]$ is the rounding operator and $\sigma^2_{\hat{N}_{k|1,\ldots,k-1}}$ denotes the conditional variance that is given by

$$\sigma^2_{\hat{N}_{k|1,\ldots,k-1}} = \sigma^2_{\hat{N}_k} - \sum_{j=1}^{k-1} \sigma^2_{\hat{N}_k \hat{N}_{j|1,\ldots,j-1}} \sigma^{-2}_{\hat{N}_{j|1,\ldots,j-1}}. \tag{32}$$

Note that the conditional ambiguity estimates are uncorrelated.

Benefit of ambiguity resolution

Fig. 1 shows the achievable accuracy of receiver and satellite phase bias estimates for a network of $R = 20$ reference stations: Ranges, range rates, ionospheric delays, ambiguities, receiver and satellite phase biases are estimated by a Kalman filter which is initialized by a least-squares solution [9]. The float ambiguities are decorrelated and sequentially fixed after 200 epochs with an error rate of less than 10^{-9}. The fixing reduces the uncertainty in the bias estimates by a factor 5. Dual frequency E1 and E5 code and carrier phase measurements from $K_r = 10$ satellites at $R = 20$ receivers have been simulated.

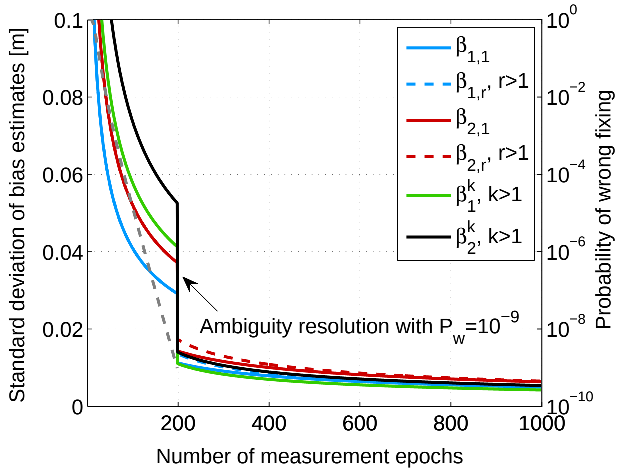

Fig. 1 Accuracy of receiver and satellite bias estimation for a network of $R = 20$ reference stations: Ranges, range rates, ionospheric delays, ambiguities, receiver and satellite phase biases are estimated by a Kalman filter which is initialized by a least-squares solution. The float ambiguities are decorrelated and sequentially fixed after 200 epochs with an error rate of less than 10^{-9}. The fixing reduces the uncertainty in the bias estimates by a factor 5.

As the bias estimation is performed on range domain, the achievable accuracy does not depend on the satellite geometry.

Benefit of a third frequency

Fig. 2 shows the benefit of measurements on a third frequency for bias estimation: If no ambiguities are fixed, the benefit of the third frequency for bias estimation remains negligible. However, the redundancy given by the third frequency enables an almost three times earlier ambiguity fixing, and, thus a higher accuracy of the bias estimates. Dual frequency E1 and E5a and triple frequency E1, E5a and E5b measurements of $R = 20$ receivers and $K_r = 10$ satellites are used for the estimation of ranges, range rates, ionospheric delays, ambiguities, receiver and satellite phase biases. Note that the code biases on the third frequency have to be estimated, as the ranges and ionospheric delays can absorb the code biases on only two frequencies. However, the absence of both ambiguities and biases on the other two code measurements (due to absorption by the range and ionospheric delay) enable a higher accuracy for the code bias estimates despite the increased code noise level.

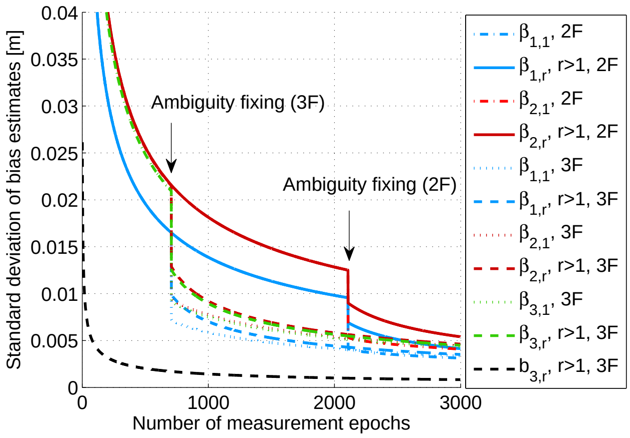

Fig. 2 Benefit of measurements on a third frequency for bias estimation: The redundancy given by the third frequency enables an almost three times earlier ambiguity fixing, and, thus a higher accuracy of the bias estimates. Dual frequency E1-E5a and triple frequency E1, E5a and E5b measurements are used for the estimation of ranges, range rates, ionospheric delays, ambiguities, receiver and satellite phase biases. Note that the code biases on the third frequency have to be estimated, as the ranges and ionospheric delays can absorb the code biases only on two frequencies.

Fig. 3 shows the achievable accuracies for the satellite phase and code biases for the same scenario. The satellite biases can be estimated with a slightly higher accuracy than the receiver biases once the ambiguities are fixed due to $R > K_r$. If no ambiguities are fixed, the receiver bias estimation benefits from the absorption of one satellite bias by the receiver biases.

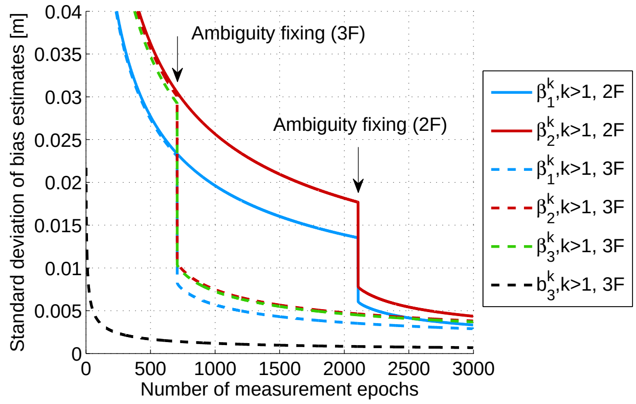

Fig. 3 Benefit of measurements on a third frequency for bias estimation: The achievable achievable accuracies are shown for the satellite biases. The same scenario as in Fig. 2 has been assumed. The redundancy given by the third frequency results in an almost three times earlier ambiguity fixing, and, thus a higher accuracy of the bias estimates.

A second Kalman filter is used to estimate the biases $\tilde{b}_{g_r}$ and $\tilde{b}_{g^k}$. The range estimates $\hat{\tilde{g}}_r^k$ of the first Kalman filter are considered as measurements which can be decomposed into

$$\begin{aligned}\tilde{g}_r^k(t_n) \;&=\; \left(\boldsymbol{e}_r^k\right)^T \cdot \left(\boldsymbol{x}_r - \boldsymbol{x}^k\right)\\ &\quad +c \cdot \left(\delta\tau_r(t_n) - \delta\tau^k(t_n)\right)\\ &\quad +T_r^k(t_n) + \tilde{b}_{g_r} + \tilde{b}_{g^k}, \qquad (33)\end{aligned}$$

where $\boldsymbol{e}_r^k$ is the unit vector from the satellite to the receiver, $\boldsymbol{x}_r$ represents the position of the reference station and $\boldsymbol{x}^k$ denotes the position of the satellite. The coordinates of the reference stations are assumed to be known and the satellite clock offset is mapped to the satellite biases $\tilde{b}_{g^k}$. Therefore, the second Kalman filter includes $\boldsymbol{x}^k(t_n)$, $c\tau_r(t_n)$, $T_r^k(t_n)$, $\tilde{b}_{g_r}$ and $\tilde{b}_{g^k}$ as state vectors. The achievable accuracies for this second Kalman filter have been shown in [9]. Note that the obtained satellite position estimates $\hat{\boldsymbol{x}}^k$ can be used to verify the satellite ephemeris from the navigation message.

It is recommended that the following biases are transmitted by an augmentation system to enable integer ambiguity resolution for absolute positioning of a multi-frequency user:

$$\hat{\beta}_{m,r}, \hat{\beta}_m^k, \hat{b}_{3,r}, \hat{b}_3^k, \hat{\tilde{b}}_{g_r}, \hat{\tilde{b}}_{g^k}. \qquad (34)$$

ESTIMATION OF CODE BIASES AND IONOSPHERIC GRID

The code biases and the Grid Ionospheric Vertical Delays (GIVD) can be estimated also without integer ambiguity resolution. In this case, it is suggested to use the code measurements on at least two frequencies and two linear combinations of time-differenced carrier phase measurements: A geometry-preserving, ionosphere-free combination which makes the range rates observable, and a geometry-free, ionosphere-preserving combination which makes the ionospheric rates observable. The measurement model is written in matrix vector as

$$
\begin{aligned}
\boldsymbol{z}_n &= \begin{bmatrix} \rho_1(t_n) \\ \rho_2(t_n) \\ \sum_{m=1}^{M} \alpha_m \lambda_m \left(\phi_m(t_{n+1}) - \phi_m(t_n)\right) \\ \sum_{m=1}^{M} \gamma_m \lambda_m \left(\phi_m(t_{n+1}) - \phi_m(t_n)\right) \end{bmatrix} \\
&= \underbrace{\begin{bmatrix} 1 & 0 & 1 & 0 \\ 1 & 0 & q_{12}^2 & 0 \\ 0 & \Delta t & 0 & 0 \\ 0 & 0 & 0 & \Delta t \end{bmatrix}}_{\mathbf{H}_n^{(2)}} \cdot \underbrace{\begin{bmatrix} \tilde{g}(t_n) \\ \dot{\tilde{g}}(t_n) \\ \tilde{I}(t_n) \\ \dot{\tilde{I}}(t_n) \end{bmatrix}}_{\mathbf{x}_n} + \mathbf{v}_n,
\end{aligned}
\tag{35}
$$

where α_m denote the weighing coefficients of the geometry-preserving, ionosphere-free combination and γ_m represent the weighting coefficients of the geometry-free, ionosphere-preserving combination.

Fig. 4 shows a $5^\circ \times 5^\circ$ grid over Europe with the EGNOS RIMS stations (red circles) [8]. The vertical ionospheric delays at the grid points (blue squares) shall be determined from the slant ionospheric delays at the pierce points (green circles). The latter ones are provided by a Kalman filter using the measurements of Eq. (35).

Let the vertical ionospheric delay at the ionospheric grid point (IGP) $(\lambda^{(l)}, \phi^{(l)})$ be denoted by $i_0^{(l)}$, the latitudinal gradient by $i_\phi^{(l)}$ and the longitudinal gradient by $i_\lambda^{(l)}$. The ionospheric vertical delay $i_0^{(l)}$ at the l-th grid point is computed by a weighted least-squares fit of the slant ionospheric delays from the surrounding pierce points, i.e.

$$
\min_{\begin{bmatrix} i_0^{(l)} \\ i_\phi^{(l)} \\ i_\lambda^{(l)} \\ b_{\mathrm{I}_1} \\ \vdots \\ b_{\mathrm{I}_R} \\ b_{\mathrm{I}^1} \\ \vdots \\ b_{\mathrm{I}^K} \end{bmatrix}} \left\| \begin{bmatrix} \tilde{I}_1^1 \\ \vdots \\ \tilde{I}_R^K \end{bmatrix} - \boldsymbol{M}\boldsymbol{H}_I \begin{bmatrix} i_0^{(l)} \\ i_\phi^{(l)} \\ i_\lambda^{(l)} \end{bmatrix} - \boldsymbol{H}_b \begin{bmatrix} b_{\mathrm{I}_1} \\ \vdots \\ b_{\mathrm{I}_R} \\ b_{\mathrm{I}^1} \\ \vdots \\ b_{\mathrm{I}^K} \end{bmatrix} \right\|_{\boldsymbol{\Sigma}^{-1}}^2
\tag{36}
$$

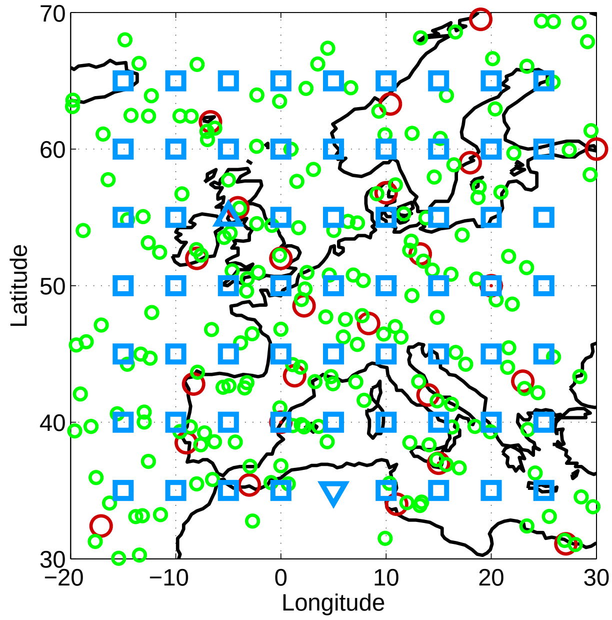

Fig. 4 Ionospheric grid: Map of Europe with EGNOS RIMS stations (red circles), ionospheric pierce points (green circles) and ionospheric grid points (blue squares) of a $5^\circ \times 5^\circ$ grid. The grid points for which the ionospheric delay can be estimated most and least accurately are also indicated.

with the mapping matrix

$$
\boldsymbol{M} = \begin{bmatrix} m_{\mathrm{I}}(E_1^1) & & \\ & \ddots & \\ & & m_{\mathrm{I}}(E_R^K) \end{bmatrix}, \tag{37}
$$

the interpolation matrix

$$
\boldsymbol{H}_I = \begin{bmatrix} 1 & \phi_1^1 - \phi^{(l)} & \lambda_1^1 - \lambda^{(l)} \\ \vdots & \vdots & \vdots \\ 1 & \phi_R^K - \phi^{(l)} & \lambda_R^K - \lambda^{(l)} \end{bmatrix}, \tag{38}
$$

the bias coefficient matrix

$$
\boldsymbol{H}_b = \left[\mathbf{1}^{R\times R} \otimes \mathbf{1}^{K\times 1},\ \mathbf{1}^{R\times 1} \otimes \mathbf{1}^{K\times K}\right], \tag{39}
$$

and the weighting matrix

$$
\boldsymbol{\Sigma} = \begin{bmatrix} \frac{\sin(E_1^1)}{\|\boldsymbol{x}_{\mathrm{IPP}_1^1} - \boldsymbol{x}_{\mathrm{IGP}^{(l)}}\|} & & \\ & \ddots & \\ & & \frac{\sin(E_R^K)}{\|\boldsymbol{x}_{\mathrm{IPP}_R^K} - \boldsymbol{x}_{\mathrm{IGP}^{(l)}}\|} \end{bmatrix}, \tag{40}
$$

where ϕ_r^k and λ_r^k denote the latitude and longitude of the ionospheric pierce point with slant delay $\tilde{I}_r^k$, $\boldsymbol{x}_{\mathrm{IPP}_r^k}$ is the position of IPP_r^k and $\boldsymbol{x}_{\mathrm{IGP}^{(l)}}$ is position of $\mathrm{IGP}^{(l)}$.

Note that the least-squares fitting of ionospheric slant delays in Eq. (36) should not use the measurements from all pierce points due to the irregular structure of the ionosphere. Typically, a bounding circle is drawn around each grid point to exclude farer points from the least-squares fitting. It has been set to 2000 km in this work. Moreover, the least-squares fitting is done jointly for all grid points as some receiver biases b_{I_r} and some satellite biases b_{I^k} occur in the estimation of several grid point delays.

Fig. 5 shows the achievable accuracy for the GIVDs. Obviously, this accuracy depends on the distribution of pierce points around the grid point. The most and least accurately computable vertical grid ionospheric delays are also indicated in Fig. 4.

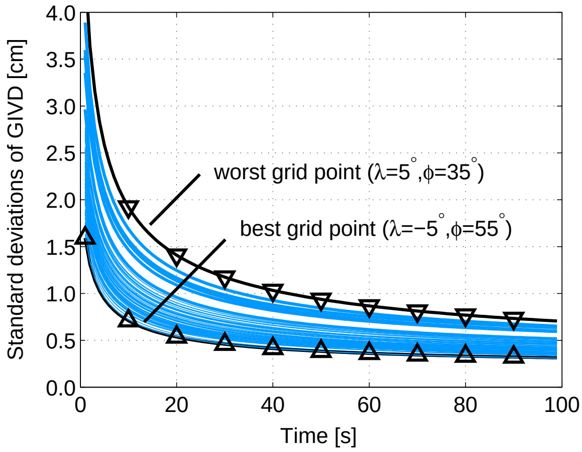

Fig. 5 Achievable accuracies for GIVD: The code measurements on E1 and E5 and two combinations of time-differenced carrier phase measurements are used in a Kalman filter to estimate the GIVD and the code biases: The first combination is geometry-preserving and ionosphere-free, and the second one is geometry-free and ionosphere-preserving which make the range rates and ionospheric rates observable respectively. A least-squares fit has been used to estimate the vertical ionospheric delay for each grid point from the slant delays of the surrounding pierce points.

MEASUREMENTS FROM CORS NETWORK

The method for joint estimation of code biases and grid ionospheric vertical delays is validated with real data from 6 CORS stations in Vermont, USA: (1) Middlebury: $\lambda = -73.15°$, $\phi = 44.00°$, (2) Montpelier: $\lambda = -72.58°$, $\phi = 44.26°$, (3) Randolph Center: $\lambda = -72.60°$, $\phi = 43.94°$, (4) Danby: $\lambda = -73.00°$, $\phi = 43.35°$, (5) Saint Johnsbury: $\lambda = -72.03°$, $\phi = 44.40°$ (6) Bradford: $\lambda = -72.11°$, $\phi = 44.01°$. The maximum distance between these 6 stations is 140 km. The GPS L1/ L2 code and carrier phase measurements of February 7, 2010 have been chosen. The ionospheric grid point at $\lambda = -71°$, $\phi = 43°$ is considered.

Fig. 6 shows the residuals of the ionospheric slant delays which are obtained from the grid estimation of Eq. (36), i.e.

$$r_I = \begin{bmatrix} \tilde{I}_1^1 \\ \vdots \\ \tilde{I}_R^K \end{bmatrix} - \boldsymbol{M}\boldsymbol{H}_I \begin{bmatrix} \hat{i}_0^{(l)} \\ \hat{i}_\phi^{(l)} \\ \hat{i}_\lambda^{(l)} \end{bmatrix} - \boldsymbol{H}_b \begin{bmatrix} \hat{b}_{\mathrm{I}_1} \\ \vdots \\ \hat{b}_{\mathrm{I}_R} \\ \hat{b}_{\mathrm{I}^1} \\ \vdots \\ \hat{b}_{\mathrm{I}^K} \end{bmatrix}. \quad (41)$$

Smaller residuals refer to the ionospheric pierce points that are closer to the grid point, and larger residuals can be observed for the ionospheric pierce points that are farer away. Consequently, these ionospheric residuals also indicate irregularities in the ionosphere. It is expected that a larger network improves the geometry and achievable accuracy.

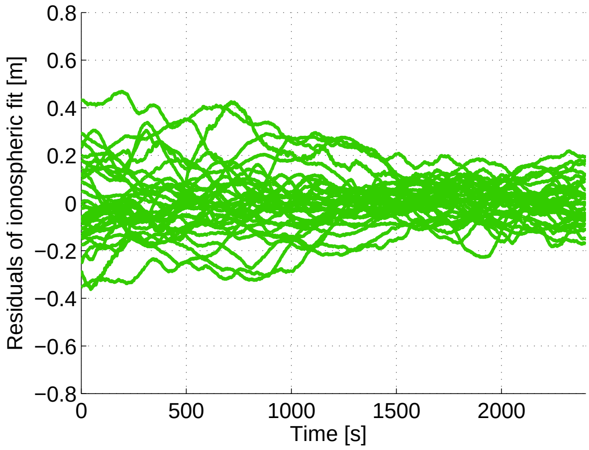

Fig. 6 Residuals of slant ionospheric delays: A least-squares fit has been used to estimate the vertical ionospheric delay for each grid point from the slant delays of the surrounding pierce points.

It is recommended that a satellite based augmentation system transmits the bias estimates $\hat{b}_{\mathrm{I}_r}$ and $\hat{b}_{\mathrm{I}^k}$ in addition to the grid ionospheric vertical delays $\hat{i}_0^{(l)}$.

INTEGER AMBIGUITY RESOLUTION WITH BIAS CORRECTIONS

Fig. 7 shows the benefit of bias estimation for integer ambiguity resolution. If no biases are corrected, a worst-case accumulation of biases over all satellites results in a poor ambiguity success rate for any of the four integer estimators: rounding, sequential fixing without or with integer decorrelation [7] and integer least-squares estimation as introduced by Teunissen [11]. The integer decorrelation transformation might amplify the biases which more than compensates for the gain obtained from the variance reduction and, thus, results in a lower success rate than rounding

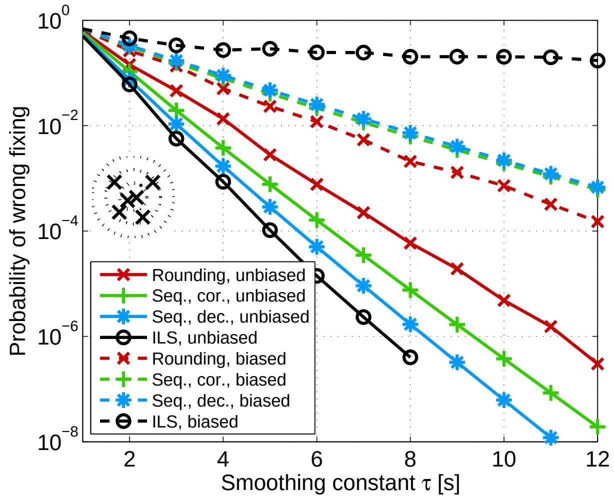

Fig. 7 Benefit of bias estimation for ambiguity resolution: The knowledge of these biases and the use of a multi-frequency widelane combination with a wavelength of several meters enables a strong reduction of the failure rate. If the biases are not estimated, a worst-case accumulation of biases over all satellites would result in substantial reduction of the ambiguity success rate.

[10][5]. An elevation dependant bias profile with a maximum code bias of 1 cm in the zenith and 10 cm in the horizon, and a maximum phase bias of 0.01 cycles in the zenith and 0.1 cycles in the horizon has been assumed as in [5].

The correction of the biases results in a substantial reduction of probability of wrong fixing. In this case, integer least-squares estimation achieves the lowest probability of wrong fixing, followed by sequential fixing with and without integer decorrelation, and rounding. A probability of wrong fixing of less than 10^{-9} can be easily achieved by a $\tau = 20$ s smoothing even for simple rounding.

CONCLUSIONS

Absolute positioning with reliable integer ambiguity resolution requires precise phase and code bias estimates. In this paper, a method for the joint estimation of satellite code, satellite phase, receiver code and receiver phase biases on multiple frequencies has been proposed. It uses a Kalman filter and sequential bootstrapping for integer ambiguity resolution. The achievable bias accuracies, the benefit of ambiguity resolution and the benefit of measurements on a third frequency have been shown for a global network of reference stations. Additionally, a second method has been suggested for joint estimation of code biases and grid ionospheric vertical delays. Code measurements on two frequencies and two linear combinations of time-differenced carrier phase measurements are used in a Kalman filter. The ionospheric delays at the grid points are obtained by a least-squares fitting of the ionospheric slant delays at the surrounding pierce points. The method has been validated from both simulated measurements of the EGNOS RIMS stations and from real data of the CORS network.

ACKNOWLEDGMENTS

The authors would like to thank the German Federal Ministry of Economic Affairs and Technology (BMWi) and the German Aerospace Center (DLR) for a financial grant (FKZ: 50NA0911) that supported this work.

REFERENCES

[1] M. Ge, G. Gendt, M. Rothacher, C. Shi and J. Liu, "Resolution of GPS carrier-phase ambiguities in Precise Point Positioning (PPP) with daily observations", *Journal of Geodesy*, Springer, pp. 389-399, Oct. 2007.

[2] M. Gabor and S. Nerem, "Satellite-satellite single difference phase calibration as applied to ambiguity resolution", *Navigation*, Journal of the Institute of Navigation, vol. 49, no. 4, pp. 223-242, 2002.

[3] D. Laurichesse and F. Mercier, "Integer ambiguity resolution on undifferenced GPS phase measurements and its application to PPP", *Proc. of ION-GNSS*, Forth Worth, USA, pp. 135-149, Sep. 2007.

[4] G. Wübbena, "GPS carrier phases and clock modeling", Lecture Notes in Earth Sciences: *GPS-Techniques Applied to Geodesy and Surveying*, vol. 19, pp. 381-392, DOI: 10.1007/BFb0011350, 1988.

[5] P. Henkel, V. Gomez and C. Günther, Modified LAMBDA for absolute carrier phase positioning in the presence of biases, *Proc. of Intern. Technical Meeting (ITM)*, Anaheim, USA, pp. 642-651, Jan. 2009.

[6] R. Brown and P. Hwang, *Introduction to random signals and applied Kalman filtering*, 3rd edition, John Wiley & Sons, New York, 1997.

[7] P. Teunissen, "Success Probability of Integer GPS Ambiguity Rounding and Bootstrapping", *Journal of Geodesy*, vol. 72, pp. 606-612, Springer, 1998.

[8] B. Arbesser-Rastburg, "Ionospheric corrections for satellite navigation using EGNOS", Proc. of XXVII-th URSI General Assembly, Maastricht, 2002.

[9] P. Henkel, Z. Wen and C. Günther, "Estimation of phase and code biases on multiple frequencies with a Kalman filter", *Proc. of 4-th Workshop on GNSS Signals and Signal Processing*, Oberpfaffenhofen, Germany, Dec. 2009.

[10] P. Teunissen, Integer estimation in the presence of biases, *Journal of Geodesy*, vol. 75, pp. 399-407, 2001.

[11] P. Teunissen, The least-squares ambiguity decorrelation adjustment: a method for fast GPS ambiguity estimation, *Journal of Geodesy*, vol. 70, pp. 65-82, 1995.